Pakistan Journal of Engineering and Technology, PakJET
Multidisciplinary | Peer Reviewed | Open Access
Volume: 03, Number: 03, Pages: 46- 50, Year: 2020

Optimization of Rao Blackwellized Particle Filter SLAM using Firefly algorithm

Muhammad Fayyaz, Muhammad Tufail, Shahzad Anwar, Zubair Ahmad and Shahbaz khan

Department of Mechatronics Engineering, University of Engineering & Technology Peshawar, Pakistan
Corresponding author: Muhammad Fayyaz (Email: 12pwmct0215@nwfpuet.edu.pk)

Abstract- **Navigation accuracy, which is an imperative performance indicator for mobile robots, is intimately associated with the grid mapping algorithm (G-mapping) accuracy. In an unstructured environment, mobile robot positioning accuracy is important to ensure safety. For this reason, in this study G-mapping Algorithm is modelled based on Rao-Blackwellized particle filter (RBPF) offering better results with a low number of sensors and features. To investigate various methods' effectiveness, a comparative analysis of three optimization methods namely Gradient descent, ANT colony, and firefly algorithm was made. The results exhibit that the firefly method performs well in terms of navigation accuracy, particle degradation, and ensuring mobile robot safety in a complex and unstructured environment**.

Index Terms-- **Machine learning, Mobile robot navigation, Optimization**.

I. INTRODUCTION

In increasingly composite and unstructured environments for mobile robots, the discovery of unidentified environments has become to be an important research area and a major concern in mobile robotics research. When a robot is in an unfamiliar location, its capability to locate itself becomes critical [1]. Furthermore, using a highly accurate global positioning system, the track detection technique use only can cause a cumulative error [2]. People expect to exploit the very important nature of multiple environmental observations while assessing the position of robots and landmarks, i.e. the location of the robot and therefore the mapping (SLAM) [3].
Simultaneous location and mapping (SLAM), which has been proposed as a tool, offers a mobile robot to travel in unknown surroundings while creating a map and assessing its position [4]. Unlike conventional navigation systems, which are based on previous environmental knowledge or external reference systems (e.g., GPS), SLAM requires the deployment of on-board sensors without additional assistance. As a result, SLAM has gained much consideration in mobile robotics and has become a key instrument for solving the problem of autonomous navigation of several unmanned vehicles, such as unmanned aerial vehicles [5], [6], under-robot marine [7], [8] and space robots [9].
SLAM is categorized into two types depending on sensors employed which are visual and LiDAR SLAM [10]. LiDAR SLAM is becoming an essential novel technique in the existing localization system due to its advantages, such as precise angle and distance measurement, the absence of scene design, multisensor fusion, the low light environment, and map generation to facilitate navigation [11]. The goal of laser SLAM is to map the environment and navigate the robot through an unstructured surrounding [12].
The robot, which incorporates light detection and range (LiDAR) as a sensor, is widely applied in commercial and civilian applications, considering the benefits of high accuracy, broad range, and transmission speed [13]–[16]. Similarly, the Robot Operating System (ROS) has many SLAM libraries such as SLAM G-mapping, Hector SLAM, ORB-SLAM, etc. [17]. Several studies on UGV robots introduces Hector SLAM [18]–[20] and LiDAR sensors. An automated motion robot was developed using a SLAM mapping algorithm that employs ROS for various obstacles detection [21].
Based on known odometry, LiDAR data, and inertial measurement unit (IMU), the mapping and localization of the G-mapping algorithm are established via modelling of Rao-Blackwellized particle filter (RBPF) [22]–[25]. Laser recognize 2D planes at different distances and angles, thereby creating information about point clouds in the spatial plane. The comparatively large map inaccuracy (i.e., navigation inaccuracy) is essential due to collective odometer errors and the effects of the RBPF algorithm (for example, high calculations and particle degradation). To enhance the accurateness of the G-mapping algorithm and lessen navigation inaccuracies, an optimization algorithm can be used to handle larger RBPF particle numbers and degradation, thereby improving particle distribution and providing particle diversity. Frequently used optimization algorithms comprise genetic algorithm, gradient descent, and firefly algorithm, ant colony algorithm [25]–[27].
To evaluate the least square problem, gradient descent algorithm was used, whereas to find an optimum path ANT colony algorithm is applied. The most extensively applied intelligent

algorithm in almost all fields is the firefly algorithm. In firefly algorithm the particle filter will be optimized intelligently, showing that the particle state is updated and particle degradation is avoided ensuring improved computational efficiency.

In this research, a comparative analysis of three well-established optimization techniques for SLAM is made. This study incorporates a differential drive robot having two LiDAR mounted on its surface. The simulation results prove that the SLAM accuracy could be improved significantly by using optimization algorithms such as firefly algorithm thereby indicating that the navigation errors can be greatly reduced as compared to the other algorithms.

II. KINEMATICS OF DIFFERENTIAL ROBOT

The differential drive has two wheels attached to a common axis so that both wheels can be moved backwards or forwards independently.

Though both wheels speed could differ, the robot needs to move around a point that is alongside the axis of each wheel. The point about which the robot whirls is Instantaneous Center of Curvature ICC as shown in Fig.1.

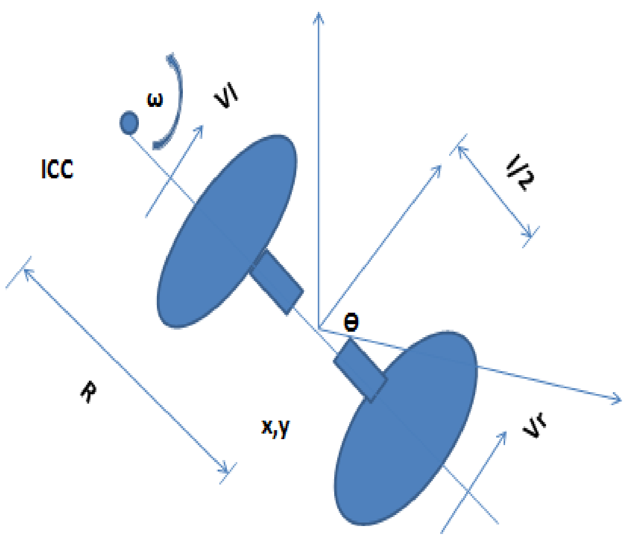

FIGURE 1. Kinematics of Differential Drive [28]

With the changing speeds of both wheels, the path that the robot takes can be changed. Because the rotation speed ω around the ICC needs to be the same for each wheel.

$$V_r = w(R + l/2) \quad (1)$$

$$V_l = w(R - l/2) \quad (2)$$

Where l is the distance among the centre of both wheels, V_r, V_l are the speeds of both wheels, whereas R is the specific distance from the ICC to the middle of the wheels. R and ω can be solved at any time:

$$R = \frac{l}{2}\frac{V_l + V_r}{V_r - V_l}\,;\, \omega = \frac{V_r - V_l}{l}; \quad (3)$$

If V_l is equal to V_r (V_l $=V_r$), then, in that case, it has a straight linear motion. R becomes zero and there is no real rotation: ω is zero. If V_l = - V_r R becomes zero then there is a rotation around the centre of the wheel axis.

If V_l = 0, then there is a rotation along with the left wheel. In this scenario, R = 1/2. This is also true when V_r is equal to zero. The next section will present the methodology employed in details.

III. METHODOLOGY

A. G-mapping

G-mapping is one of the most accepted SLAM algorithms in robotics. To sort out laser data it uses a filter along with a Rao-Blackwellized particle filter. Then it takes into account the altered movement and new observations of the robot.The overall methodology is presented in Fig. 2.

In this way, the algorithm reduces the probability of robots pose uncertainty in the prediction of filtering. Besides, it selectively performs repetitive sampling operations, reducing the setback of particle depletion.

For SLAM the basic idea of the Rao-Blackwellized particle filter is to calculate the posterior probability $p(x_{1:t}|z_{1:t} \quad u_{0:t})$ regarding probable trajectories $x_{1:t}$ of a robot based on its observations $z_{1:t}$ and Odometery measurements $u_{o:t}$ and to make use of it posterior to calculate posterior in trajectories and maps.

$$p(x_{1:t}, \quad m|z_{1:t}, \quad u_{0:t}) = p(m|x_{1:t}, \quad z_{1:t})p(x_{1:t}|z_{1:t} \quad u_{0:t}) \quad (4)$$

To calculate the posterior $p(x_{1:t}|z_{1:t} \quad u_{0:t})$ in possible trajectories, Rao-Blackwellized uses a particle filter where each map is related to each sample. Each map is constructed based on the observations $z_{1:t}$ and path $x_{1:t}$ represented by the subsequent particle. The robot's trajectory changes with the movement of the robot. And due to this reason, the proposal distribution is selected equal to the probabilistic Odometric motion pattern. For Incremental mapping Rao-Blackwellized SIR (Sampling Importance Resampling) filter processes the available observations and Odometer readings. This was performed employing updating a set of samples representing the subsequent posterior concerning the maps as well as vehicle trajectories.

1) Sampling

To get next-generation particles $\left\{x_t^{(i)}\right\}$ from the current generation $\left\{x_{t-1}^{(i)}\right\}$ is done through sampling from a proposal distribution$\pi(x_t|z_{1:t}, \quad u_{0:t})$.

2) Importance weighting

Each particle is assigned a weight based on its importance,

$$w^{(i)} = \frac{p\left(x_t^{(i)} \middle| z_{1:t}, \quad u_{0:t}\right)}{\pi\left(x_t^{(i)} \middle| z_{1:t}, \quad u_{0:t}\right)} \qquad 4(i)$$

This implies the fact that the proposed distribution in common is not identical to the proper distribution of successor states.

3) Resampling

A sample of high weight w particles normally replaces particles having low importance regarding the weights. This is a necessary step because simply a limited amount of particles are utilized to estimate a constant distribution. Moreover, in situations where the exact distribution differs from the proposed, Resampling allows applying particle filter.

4) Estimating Map

The consequent map estimate $m_t^{(i)}$ for each pose sample $x_t^{(i)}$ is calculated depending on the path and the past of observations: $p\left(m_t^{(i)} \middle| x_{1:t}^{(i)}, \quad z_{1:t}\right)$.

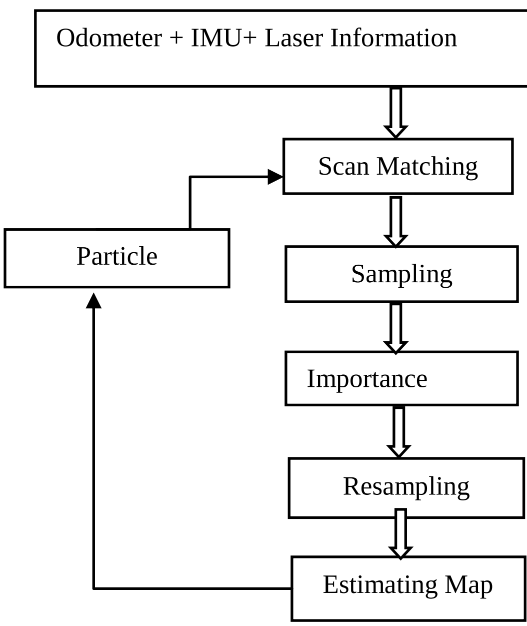

FIGURE 2. Flowchart of RBPF

B. Firefly Algorithm

The rules that the firefly algorithm follows are as follows: The relative brightness between fireflies can be expressed by the following formula:

$$I = I_0 \times e^{-\gamma r_{ab}} \qquad (5)$$

Where I shows the value of the highest brightness of the firefly, γ represents the light intensity absorption coefficient, which decreases as the distance increases, and r_{ab} is the spatial distance among fireflies. The attraction formula between fireflies is described as:

$$= \beta_0 \times e^{-\gamma r_{ab}^2} \qquad (6)$$

Where β_0 show the maximum firefly attraction.

At the time when fireflies a and b are attracted to each other, the update formula is expressed as:

$$x_a = x_b + \beta \times (x_b - x_a) + \alpha \times \langle rand - \frac{1}{2} \rangle \qquad (7)$$

Where α represents the step factor while rand is a random number whose value range is between 0 and 1.

Brightness and attractiveness are the two key parameters that the firefly contains. The position and direction of firefly are determined by the brightness, while the attraction shows the range of movement of firefly. Particle optimization is achieved by continuously updating brightness and attraction.

C. Improved Firefly Algorithm

In the firefly algorithm, the position update is computationally very expensive, this is not favourable for the performance efficiency of the algorithm. The attraction among particles a and b must be recalculated in every position update with the highest attraction, distance, absorption coefficient of light intensity as well as other features. Here In this research, an enhanced idea employing global optimal particles to interrelate with each other is proposed [29]. Computationally complexity can be reduced efficiently by this idea.

The sampled particles are taken as individual fireflies, and the firefly brightness is taken as the existing particle weight.

$$\beta = \beta_0 \times e^{-\gamma r_a^2} \qquad (8)$$

Where r_a represents the distance among particles a and$pbest_t$, β_0 shows maximum attraction and γ is the maximum light intensity absorption coefficient.

$$x_t^{(a)} = x_t^{(a)} + \beta \times \left(pbest_t - x_t^{(a)}\right) + \alpha \times \langle rand - \frac{1}{2} \rangle \qquad (9)$$

Where $x_t^{(a)}$ represents the particle state value at time t, β is particle maximum attraction, α represents the step factor, rand is a random whole number ranging between between 0 and 1 and $pbest_t$ represents global optimal particle.

IV. RESULTS

Grip map matching information is analyzed using three different optimization techniques. And comparative analysis is being drawn among them. The predicted scanned point cloud in the grid map is compared with the known point cloud dataset [29]. Column vector is calculated as the distance matrix from ineffective point cloud to the existing point cloud, a dimension of which is 5500, maximum attraction (β_0) is 1, step factor (α) is 0.001, Υ (light intensity absorption coefficient) is 1, Number of particles of RBFP are 20 and number of firefly iterations is 10. The overlap ratio of a match can be attained by summing the distance matrix which is also called an evaluation function. The distance is inversely proportional to overlap ratio of two maps i.e. smaller distance will result in a higher overlap ratio. Particle overlap ratio by applying the gradient descent algorithm is shown in Fig. 3. Figure 4 shows Particle overlap ratio by ANT colony algorithm.

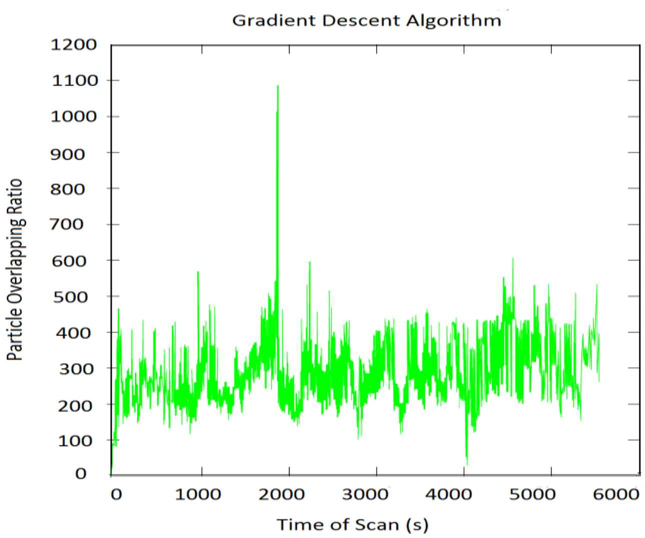

FIGURE 3. Particle overlap ratio by applying a Gradient Descent Algorithm

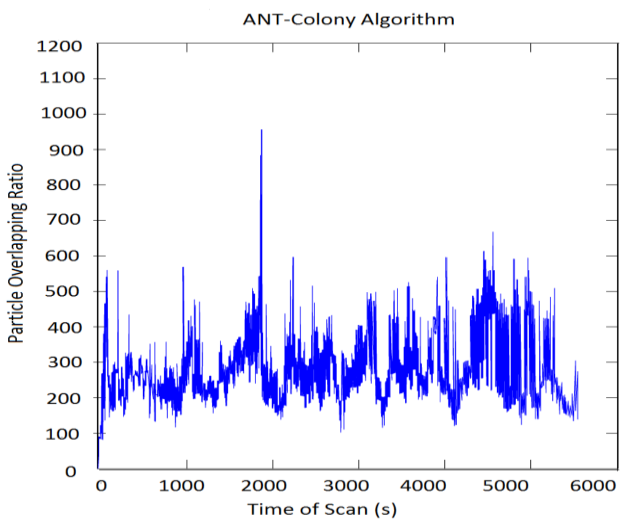

FIGURE 4. Particle overlap ratio by ANT Colony Algorithm

Similarly the result in Fig. 5 shows Particle overlap ratio by firefly algorithm. A Comparison between all algorithms for particle overlap ratio is shown in Fig 6.

The results shown in Fig. 6 exhibits that employing firefly algorithm, the overlap ratio of particles is reasonably small which have a positive implication on the matching effect of the map as well as enhancing G-mapping capacity. The optimization technique have many real world applications such as, for instance ,employing mobile robots in search and rescue operations, unmanned vehicle (UAV) deployment in precision agriculture for spraying, underwater robot navigation for mineral exploration etc. In this study, mobile robot particle degradation and state estimation accuracy have been improved via G-mapping modelling, on the basis of Rao-Blackwellized particle filter. For this reason, a comparative analysis of three different optimization techniques namely gradient descent, ANT colony, and firefly algorithm techniques were chosen for investigation.

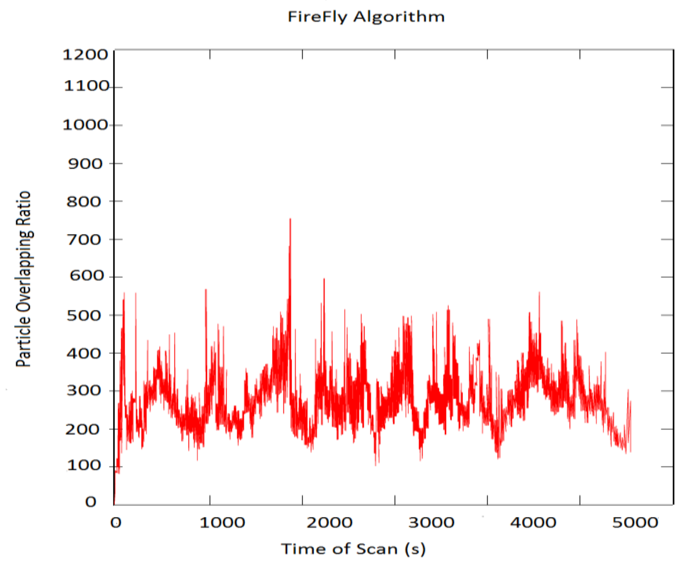

FIGURE 5. Particle overlap ratio by applying FireFly algorithm

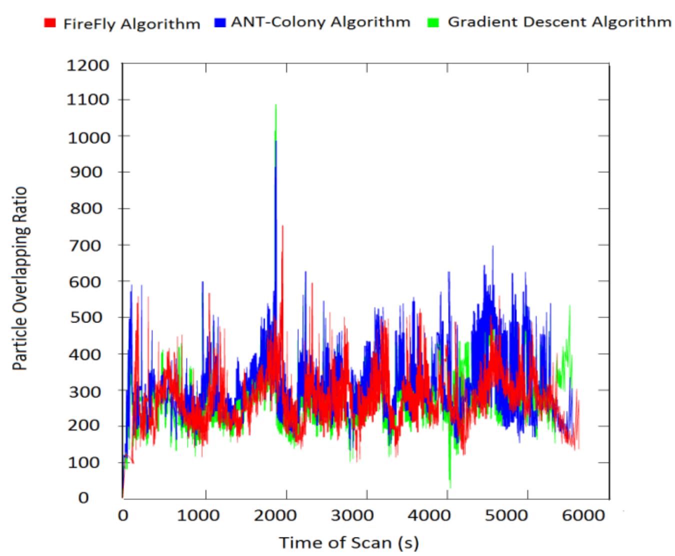

FIGURE 6. Comparison between all algorithms for particle overlap ratio.

All the above mention techniques exhibits decent results employing Rao-Blackwellized Particle filter, however firefly algorithm shows extended performance in reducing navigation inaccuracy, particle degradation, reducing the number of particles, and ensuring mobile robot safety in a challenging and unstructured environment. In future, an investigation on feedback loop closure for navigation map accuracy is in progress.

REFERENCES

[1] J. J. Leonard and H. F. Durrant-Whyte, “Mobile Robot Localization by Tracking Geometric Beacons,” IEEE Trans. Robot. Autom., vol 7, pp 3-382, Jun 1991.

[2] R. Ban, K. Kaji, K. Hiroi and N. Kawaguchi, "Indoor positioning method integrating pedestrian Dead Reckoning with magnetic field

and WiFi fingerprints," 2015 Eighth International Conference on Mobile Computing and Ubiquitous Networking (ICMU), Hakodate, 2015, pp. 167-172, doi: 10.1109/ICMU.2015.7061061..

[3] R. Smith, M. Self, and P. Cheeseman, "Estimating Uncertain Spatial Relationships in Robotics," in *Machine Int. and Pat. Recog.*, vol 5, pp 435-461 1988.

[4] H. Durrant-Whyte and T. Bailey, "Simultaneous localization and mapping: Part I," *IEEE Robot. Autom. Mag.*, vol 13, pp 99-110, June 2006.

[5] F. Caballero, L. Merino, J. Ferruz, and A. Ollero, "Vision-based odometry and SLAM for medium and high altitude flying UAVs," *J. Intell. Robot. Syst. Theory Appl.*, vol 54, pp 137-161, 2009.

[6] C. L. Wang, T. M. Wang, J. H. Liang, Y. C. Zhang, and Y. Zhou, "Bearing-only visual SLAM for small unmanned aerial vehicles in GPS-denied environments," *Int. J. Autom. Comput.*, vol 10, pp 387-396, July 2013.

[7] A. Mallios, P. Ridao, D. Ribas, and E. Hernández, "Scan matching SLAM in underwater environments," *Auton. Robots*, vol 36, pp 181-198 2014.

[8] C. S. Lee, S. Nagappa, N. Palomeras, D. E. Clark, and J. Salvi, "SLAM with SC-PHD filters: An underwater vehicle application," *IEEE Robot. Autom. Mag.*, vol 21, pp 38-45, May 2014.

[9] C. H. Tong, T. D. Barfoot, and E. Dupuis, "Three-dimensional SLAM for mapping planetary work site environments," in *J. of Field Rob.*, vol 29, pp 381-412, 2012.

[10] M. J. Segura, F. A. A. Cheein, J. M. Toibero, V. Mut, and R. Carelli, "Ultra Wide-Band localization and SLAM: A comparative study for mobile robot navigation," *Sensors*, vol 11, pp 2035-2055, 2011.

[11] Dong Shen, Yuhang Xu, and Yakun Huang. 2019. Research on 2D-SLAM of Indoor Mobile Robot based on Laser Radar. *In Proceedings of the 2019 4th International Conference on Automation, Control and Robotics Engineering (CACRE2019). Association for Computing Machinery, New York, NY, USA*, Article 64, 1–7. DOI:https://doi.org/10.1145/3351917.3351966.

[12] T. Zheng, C. Meng, P. Zou and J. Wang, "Improvement of Gmapping Algorithm Based on Non-continuous System," 2019 Chinese Control And Decision Conference (CCDC), Nanchang, China, 2019, pp. 5058-5063, doi: 10.1109/CCDC.2019.8833316.

[13] G. W. Y. Cheng, "'Mobile Robot Navigation Based on Lidar,'" in *Chinese Control And Decision Conference.IEEE*, 2018, pp. 1243–1246.

[14] J. Park, J. Y. Kim, B. C. Kim, and S. Kim, "Global Map Generation using LiDAR and Stereo Camera for Initial Positioning of Mobile Robot," in *2018 International Conference on Information and Communication Technology Robotics*, pp 1-4, 10.1109/ICT-ROBOT.2018.8549897.

[15] S. Ghorpade, Deepali and Thakare, Anuradha D and Doiphode, "Obstacle Detection and Avoidance Algorithm for Autonomous Mobile Robot using 2D LiDAR," in *International Conference on Computing, Communication, Control and Automation (ICCUBEA)*, pp. 1-6, 10.1109/ICCUBEA.2017.8463846.

[16] R. Li, J. Liu, L. Zhang, and Y. Hang, "LIDAR/MEMS IMU integrated navigation (SLAM) method for a small UAV in indoor environments," in *2014 DGON Inertial Sensors and Systems (ISS)*, 2014, pp. 1–15.

[17] Y. Pyo, R. Kurazume, and Y. Watanabe, "ROS Robot Programming," vol. Republic o, p. 342,

[18] S. Kohlbrecher, O. Von Stryk, J. Meyer, and U. Klingauf, "A flexible and scalable SLAM system with full 3D motion estimation," in *9th IEEE International Symposium on Safety, Security, and Rescue Robotics, SSRR 2011*, 10.1109/SSRR.2011.6106777.

[19] K. O. Arras, S. Grzonka, M. Luber and W. Burgard, "Efficient people tracking in laser range data using a multi-hypothesis leg-tracker with adaptive occlusion probabilities," 2008 *IEEE International Conference on Robotics and Automation, Pasadena, CA, 2008*, pp. 1710-1715, doi: 10.1109/ROBOT.2008.4543447. .

[20] I. Z. Ibragimov and I. M. Afanasyev, "Comparison of ros-based visual slam methods in homogeneous indoor environment," in *2017 14th Workshop on Positioning, Navigation and Communications (WPNC)*, 2017, pp. 1–6, 10.1109/WPNC.2017.8250081.

[21] B. L. E. A. Balasuriya *et al.*, "Outdoor robot navigation using Gmapping based SLAM algorithm," in *2nd International Moratuwa Engineering Research Conference, MERCon 2016*, 10.1109/MERCon.2016.7480175.

[22] R. P. Guan, B. Ristic, and L. Wang, "Combining KLD-sampling with Gmapping proposal for grid-based Monte Carlo localization of a moving robot," in *20th International Conference on Information Fusion, Fusion 2017 - Proceedings*, 10.23919/ICIF.2017.8009684.

[23] G. Grisetti, C. Stachniss, and W. Burgard, "Improving grid-based SLAM with Rao-Blackwellized particle filters by adaptive proposals and selective resampling," in *Proceedings - IEEE International Conference on Robotics and Automation*, doi: 10.1109/ROBOT.2005.1570477.

[24] G. Grisetti, C. Stachniss, and W. Burgard, "Improved techniques for grid mapping with Rao-Blackwellized particle filters," *IEEE Trans. Robot.*, 2007, pp. 2432-2437, doi: 10.1109/ROBOT.2005.1570477.

[25] M. Chen, C. Bian, and Y. J. Wu, "Research on Rao-Blackwillised Particle Filter SLAM algorithm based on QPSO," in *2018 37th Chinese Control Conference (CCC)*, 2018, pp. 5179–5185, doi: 10.23919/ChiCC.2018.8483359.

[26] L. Qing, Z. Chao, X. Yinmei, and Y. Yixin, "Path planning of mobile robots based on specialized genetic algorithm and improved particle swarm optimization," in *Proceedings of the 31st Chinese Control Conference*, 2012, pp. 7204–7209.

[27] J. W. Lee, B. S. Choi, K. T. Park, and J. J. Lee, "Comparison between heterogeneous ant colony optimization algorithm and Genetic Algorithm for global path planning of mobile robot," in *Proceedings 2011 IEEE International Symposium on Industrial Electronics*, 2011, pp 881-886, doi: 10.1109/ISIE.2011.5984275.

[28] G. Dudek and M. Jenkin, *Computational Principles of Mobile Robotics*. 2010 .

[29] R. Wu, L. Shu, and X. Zhao, "Optimization of the Grid Mapping Algorithm for Mobile Robots," in *Journal of Physics: Conference Series*, 2019, (vol. 1237, no. 2, p. 22074) IOP Publishing, doi.org/10.1088/1742-6596/1237/2/022074